Available online at www.sciencedirect.com
ScienceDirect
Nuclear Physics B Proceedings Supplement 00 (2014) 1–6
Nuclear Physics B Proceedings Supplement

Search for the Higgs boson in VH(bb) channel using the ATLAS detector

Paolo Francavilla, on behalf of the ATLAS Collaboration

Laboratoire de Physique Nucléaire et de Hautes Energies and Institut Lagrange de Paris, CNRS/IN2P3, Paris, France

Abstract

Since the discovery of a Higgs boson by the ATLAS and CMS experiments at the LHC, the emphasis has shifted towards measurements of its properties and the search for less sensitive channels in order to determine whether the new particle is the Standard Model (SM) Higgs boson. Of particular importance is the direct observation of the coupling of the Higgs boson to b-quarks. In this talk a review of ATLAS results in the search for the Higgs boson in the VH production mode with the Higgs decaying to a b-quark pair will be given.

Keywords: Higgs physics, Associated production, B-quarks, Jets

1. Introduction

Since the observation of a new particle by the ATLAS and CMS experiments at the LHC [1, 2] with properties consistent with the Higgs boson [3, 4, 5, 6] of the Standard Model (SM) [7, 8, 9], the emphasis has shifted towards precise measurements of its properties and the study of less sensitive channels.

The $H \to b\bar{b}$ decay mode is predicted in the SM to have a branching ratio of 58% for $m_H = 125$ GeV [10].

These proceedings describe the details of the analysis performed by the ATLAS collaboration in the search for associated $(W/Z)H$ production of the SM Higgs boson in the $b\bar{b}$ decay. The associated production of a Higgs boson with a vector boson W or Z, thanks to their leptonic decays, offers a way to suppress the overwhelming background from multijet production which makes the inclusive $H \to b\bar{b}$ channel not feasible at hadron colliders.

The ATLAS experiment reported other searches for associated $(W/Z)H$ production of the SM Higgs boson in the $b\bar{b}$ decay mode, based on datasets of 4.7 and 13.0 fb^{-1} recorded at $\sqrt{s} = 7$ and 8 TeV, respectively [11, 12]. In these proceedings the search uses the full integrated luminosity accumulated by ATLAS [13] during Run 1 of the LHC, 4.7 and 20.3 fb^{-1} at centre-of-mass energies of 7 and 8 TeV in 2011 and 2012, respectively. A more complete description of the analysis can be found in [14]. Recently, a revisited and improved version of the analysis described in these proceedings has been reported by the collaboration [15].

Analysis strategy. The analysis is performed for events containing zero, one, or two charged leptons (electrons or muons), addressing the $Z \to \nu\nu$, $W \to l\nu$, or $Z \to ll$ decay modes of the vector boson, respectively. The 0-lepton channel has a reduced but not negligible contamination from $W \to l\nu$, when the lepton is produced outside of the detector acceptance or not identified.

A b-tagging algorithm is used to identify the jets from the $H \to b\bar{b}$ decay. To improve the sensitivity, the three channels are further split according to the vector boson transverse momentum and the number of jets, and topological and kinematic selection criteria are applied within each of the resulting categories.

In the statistical analysis used to obtain the final results, the mass of the two b-tagged jets is used as the discriminating variable, and dedicated control samples constrain the contributions of the dominant background processes.

To validate the analysis, a measurement of the cross section of $(W/Z)Z$ production is performed in the same final states and with the same event selection, with $H \to b\bar{b}$ replaced by $Z \to b\bar{b}$.

2. Object definition and event selection

The analysis uses the full integrated luminosity accumulated by ATLAS during Run 1 of the LHC, 4.7 and 20.3 fb^{-1} at centre-of-mass energies of 7 and 8 TeV in 2011 and 2012, respectively. Single-lepton triggers and dilepton triggers have been used to select events for the 1-lepton channel and the 2-lepton channel. Events in the 0-lepton channel are selected by triggers based on missing transverse momentum ($E_{\mathrm{T}}^{\mathrm{miss}}$). In addition, $E_{\mathrm{T}}^{\mathrm{miss}}$ triggers are also used to cope with a reduced muon-chamber coverage in some regions of the detector, thus improving the signal acceptance by about 20% in the muon channel for the 1-lepton analysis.

The object definition is summarised in the following lines:

Leptons Three categories of electrons [16] and muons [17] are used in the analysis, denoted in increasing order of purity as loose, medium and tight leptons which differ for quality and isolation requirements. Loose leptons are selected with transverse energy $E_{\mathrm{T}} > 10$ GeV and $|\eta| < 2.5$ ($|\eta| < 2.47$ for electrons). Medium leptons meet the loose identification criteria and have $E_{\mathrm{T}} > 25$ GeV, and they pass additional quality requirements. Tight leptons are required to pass still more stringent quality and isolation requirements based on variables measured by the tracking system and by the calorimeters.

Jets Jets are reconstructed from topological clusters in the calorimeters using the anti-k_{t} algorithm [18] with a distance parameter of 0.4 [19]. To reduce the contamination by jets from pile-up interactions, a criterion using the ratio between the scalar sum of the p_T of tracks matched to the jet and originating from the primary vertex and the scalar sum of the p_T of all tracks matched to the jet has been used. Jets with $p_{\mathrm{T}} > 20$ GeV and $|\eta| < 2.5$ have been considered to build the dijet system representing the Higgs candidate (adding the request that the highest p_{T} jet must have $p_{\mathrm{T}} > 45$ GeV), while extra jets with $p_{\mathrm{T}} > 30$ GeV and $2.5 < |\eta| < 4.5$ have been used in the 0-lepton and in the 1-lepton channel to veto the event.

***b*-tagging** Jets originating from b-quarks are identified using the MV1 b-tagging algorithm [20], which combines information from various algorithms based on track impact-parameter significance or explicit reconstruction of b-hadron decay vertices. The b-tagging selection criterion used in this analysis results in a typical efficiency of 70% for b jets, as measured in simulated $t\bar{t}$ events, and rejection factors of 5 and 150 against c and light jets, respectively.

$E_{\mathrm{T}}^{\mathrm{miss}}$ and $p_{\mathrm{T}}^{\mathrm{miss}}$ The missing transverse momentum $E_{\mathrm{T}}^{\mathrm{miss}}$ [21] is measured as the negative vector sum of the transverse momenta associated with electrons, photons, muons, taus and jets in the event. The transverse momenta associated with the energy clusters in the calorimeters with $|\eta| < 4.9$ not associated with any reconstructed object, is used to improve the estimate of the $E_{\mathrm{T}}^{\mathrm{miss}}$. In addition, a track-based missing transverse momentum, $p_{\mathrm{T}}^{\mathrm{miss}}$, is calculated as the negative vector sum of the transverse momenta of tracks associated to the primary vertex.

Signal region. The basic event selection for the three channels is summarised in Table 1. The transverse momentum of the vector boson (p_{T}^{V}) is reconstructed as the $E_{\mathrm{T}}^{\mathrm{miss}}$ in the 0-lepton channel, the magnitude of the vector sum of the lepton and the $\vec{E}_{\mathrm{T}}^{\mathrm{miss}}$ in the 1-lepton channel (p_{T}^{W}) and of the vector sum of the two leptons in the 2-lepton channel (p_{T}^{Z}). The events are categorised in five p_{T}^{V} intervals, with boundaries at 0, 90, 120, 160, and 200 GeV. The $E_{\mathrm{T}}^{\mathrm{miss}}$triggers are 90% efficient for $E_{\mathrm{T}}^{\mathrm{miss}}$= 120 GeV, so only the last three intervals are used in the 0-lepton channel.

The events are selected if there are exactly two b-tagged jets with $|\eta| < 2.5$. In addition, the leading (highest p_{T}) b-tagged jet must have $p_{\mathrm{T}} > 45$ GeV. The dijet system is formed by these two b-tagged jets. There can be at most one additional jet with $p_{\mathrm{T}} > 20$ GeV and $|\eta| < 2.5$.

Additional requirements applied on the angular separation $\Delta R(b, \bar{b})$ between the two jets of the dijet system have been used. These cuts have been optimized in different p_{T}^{V} interval, to improve the background-signal separation ($\Delta R(b, \bar{b}) > 0.7$ if $p_{\mathrm{T}}^{V} < 200$ GeV,

Table 1: The basic event selection for the three channels. In this table, $\Delta\phi(\vec{E}_{\mathrm{T}}^{\mathrm{miss}}, \vec{p}_{\mathrm{T}}^{\mathrm{miss}})$ is the azimuthal angle between $\vec{E}_{\mathrm{T}}^{\mathrm{miss}}$and $\vec{p}_{\mathrm{T}}^{\mathrm{miss}}$, $\Delta\phi(\vec{E}_{\mathrm{T}}^{\mathrm{miss}}, \mathrm{j})$ is the azimuthal angle between $\vec{E}_{\mathrm{T}}^{\mathrm{miss}}$and a jet j in the event, $\Delta\phi(\vec{E}_{\mathrm{T}}^{\mathrm{miss}}, b\bar{b})$ is the azimuthal angle between $\vec{E}_{\mathrm{T}}^{\mathrm{miss}}$and the dijet system forming the Higgs candidate, $m_{\mathrm{T}}^{W}$is the transverse mass built from the lepton kinematic and the $\vec{E}_{\mathrm{T}}^{\mathrm{miss}}$, and $m_{\ell\ell}$is the dilepton invariant mass.

0-lepton	1-lepton	2-lepton
0 loose leptons	1 tight lepton	1 medium lepton
	+ 0 loose leptons	+ 1 loose lepton
$E_{\mathrm{T}}^{\mathrm{miss}}$/[GeV] > 120	$E_{\mathrm{T}}^{\mathrm{miss}}$/[GeV]> 25	$E_{\mathrm{T}}^{\mathrm{miss}}$/[GeV]< 60
$p_{\mathrm{T}}^{\mathrm{miss}}$/[GeV] > 30	($E_{\mathrm{T}}^{\mathrm{miss}}$/[GeV]> 50	83 < $m_{\ell\ell}$/[GeV]< 99
$\Delta\phi(\vec{E}_{\mathrm{T}}^{\mathrm{miss}}, \vec{p}_{\mathrm{T}}^{\mathrm{miss}}) < \pi/2$	if p_{T}^{W}/[GeV] > 200)	
$\min[\Delta\phi(\vec{E}_{\mathrm{T}}^{\mathrm{miss}}, \mathrm{j})] > 1.5$	m_{T}^{W}/[GeV] < 120	
$\Delta\phi(\vec{E}_{\mathrm{T}}^{\mathrm{miss}}, b\bar{b}) > 2.8$	(and m_{T}^{W}/[GeV]> 40	
	if p_{T}^{W}/[GeV]< 160)	

and $\Delta R(b,\bar{b}) < 3.4$ and decreased to 3.0, 2.3, 1.8, 1.4 if p_{T}^{V}/[GeV] > 90, 120, 160, 200 respectively). These selection criteria define a set of "2-tag signal regions", categorised in terms of channel (0-, 1-, or 2-leptons), p_{T}^{V} interval, and jet multiplicity (2 or 3).

After event selection, the dijet mass is recomputed in the 2-tag regions with an improved jet calibration. The energy from muons within a jet is added to the calorimeter-based jet energy, and a p_{T}-dependent correction is applied to account for biases in the response due to resolution effects.

Some examples for the dijet mass distributions in the signal regions for the thee different lepton channels are shown in Figure 1.

Control regions. A number of "control" regions are also used in the analysis to constrain the main backgrounds. These control regions are selected in the same way as the signal regions, except for the following modifications. For the 1-tag control regions, exactly one jet must be b tagged, while for the 0-tag control region, no jet is b tagged. In the 2-lepton channel, two additional 2-tag regions are defined, which are inclusive in jet multiplicity (≥ 2). In the first one, a "validation region", the requirement on the dilepton mass is reversed ($40 < m_{\ell\ell} < 83$ GeV or $m_{\ell\ell} > 99$ GeV) and no requirement is placed on $E_{\mathrm{T}}^{\mathrm{miss}}$. In the second one, a "control region", events containing different-flavour lepton pairs (electron or muon) are selected.

3. Estimate of the background, systematic uncertainties and fit strategy

As shown in Figure 1 most of the electroweak processes including jets enter as background in this analysis. It can be seen that the background composition in the signal regions varies greatly from channel to channel, with the jet multiplicity, and with the p_{T}^{V} interval considered. The signal to background ratio improves with increasing p_{T}^{V}. Their contribution have been estimated by using Monte Carlo (MC) simulated samples produced using the ATLFAST-II simulation [22], which includes a full simulation of the ATLAS detector based on the GEANT4 program [23], except for the response of the calorimeters for which a parametrised simulation is used. For the main background processes, version 1.4.1 of the SHERPA generator [24] to simulate W and Z+jets at leading-order (LO) in QCD, with massive c and b quarks has been used. The $t\bar{t}$ production has been simulated with the POWHEG generator [25, 26, 27], interfaced with PYTHIA6 [28]. For single-top, POWHEG,and AcerMC generator [29] have been used. The HERWIG

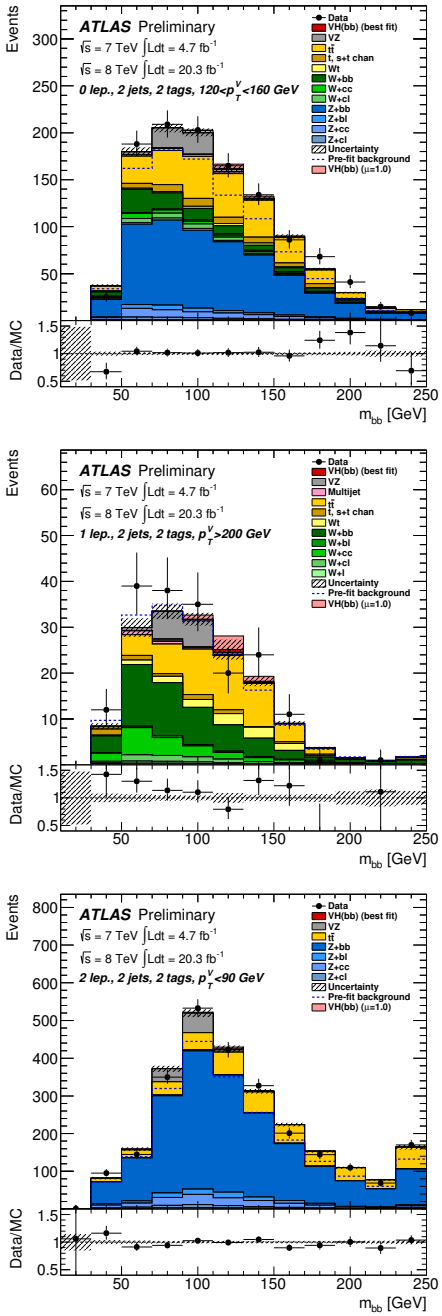

Figure 1: The m_{bb} distribution in data (points with error bars) and simulation (histograms) for the six signal regions of the 0-lepton, 1-lepton and 2-lepton channel [14]. The background contributions after the global fit are shown as filled histograms. The Higgs boson signal ($m_H = 125$ GeV) is shown as filled histograms on top of the fitted backgrounds both after the global fit (indicated as "best fit") and as expected from the SM (indicated as $\mu = 1.0$). The size of the combined statistical and systematic uncertainty on the fitted signal+background is indicated by the hashed band. The dashed blue histogram shows the total background as expected from the pre-fit Monte Carlo simulation. The entries in overflow are included in the last bin.

generator [30] is used for diboson processes. The multijet background is estimated from data in each of the 0-, 1-, and 2-lepton channels, and of the 2- and 3-jet, 0-, 1-, and 2-tag regions.

Because of the importance of the precise determination of the background contribution to the measured m_{bb} distributions, a detailed campaign of studies has been done to determine corrections and systematic uncertainties on the modelling of each background. In particular, rescaling factors have been obtained from the global fit (described in *Statistical interpretation*) to the 7 TeV + 8 TeV data for the normalisation of the most prominant backgrounds: $t\bar{t}$, Wb, Wcl, Zb, and Zcl. For all the other processes, the status-of-the-art perturbative calculations have been used to determine the contribution to the background.

The MC generator used for the WH and ZH signal processes is PYTHIA8 [31]. The total production cross sections and associated uncertainties are computed at next-to-next-to-leading order (NNLO) in QCD[1] and with electroweak corrections at next-to-leading order (NLO) according to Refs. [33, 34, 35, 36]. Additional NLO corrections are applied as a function of the transverse momentum of the vector boson [37]. The decay branching ratios are calculated with HDECAY [10]. Signal samples are simulated for Higgs boson masses from 100 to 150 GeV in steps of 5 GeV.

The impact of the uncertainties due to the object reconstruction has been evaluated on the signal and on the background. The uncertainties can be divided in the ones from the performance of the electrons, muons, jets, $E_{\mathrm{T}}^{\mathrm{miss}}$ b-tagging, and trigger. Among the others, the one on jets, and b-tagging seems to play a bigger role in the analysis.

Statistical interpretation. The statistical analysis of the data employs a binned likelihood function $\mathcal{L}(\mu, \vec{\theta})$ constructed as the product of Poisson probability terms. The inputs to the "global fit" are, for each data taking period, the m_{bb} distributions in the 26 2-tag signal regions. Additional inputs are the event yields in the top control region of the 2-lepton channel based on the $e\mu$ selection, and in the 26 1-tag control regions.

A signal strength parameter, μ, multiplies the expected SM Higgs boson production cross section. The impact of systematic uncertainties on the signal and background expectations is described by nuisance parameters, $\vec{\theta}$, which are parametrised by Gaussian prior or log-normal prior. The expected numbers of signal and background events in each bin are functions of $\vec{\theta}$. The test statistics q_μ is then constructed according to the profile likelihood ratio: $q_\mu = -2\ln(\mathcal{L}(\mu, \hat{\hat{\vec{\theta}}}_\mu)/\mathcal{L}(\hat{\mu}, \hat{\vec{\theta}}))$, where $\hat{\mu}$ and $\hat{\vec{\theta}}$ are the parameters that maximise the likelihood (with the constraint $0 \leq \hat{\mu} \leq \mu$), and $\hat{\hat{\vec{\theta}}}_\mu$ are the nuisance parameter values that maximise the likelihood for a given μ. This test statistics is used to measure the compatibility of the background-only hypothesis with the observed data and for exclusion intervals derived with the CL_s method [38, 39].

The normalisations of the $t\bar{t}$, Wb, Wcl, Zb, and Zcl backgrounds are allowed to float freely in the fit. Depending on the size of the multijet background contribution in each region, its normalisation floats freely or within its prior. The normalisations of the other backgrounds are constrained within their uncertainties.

4. Results and conclusions

Diboson production with a Z boson decaying to a pair of b-quarks and produced in association with either a W or Z boson has a signature very similar to the one considered in this analysis, but with a cross section of about five times the SM Higgs boson one. A separate fit is therefore performed as a validation of the analysis procedure. In this "Diboson fit", the normalisation of the diboson contributions is allowed to vary with a multiplicative scale factor μ_{VZ} with respect to the SM expectation, except for the small contribution from WW production, which is treated as a background and constrained within its uncertainty. A SM Higgs boson with $m_H = 125$ GeV is included as a background, with a production cross section at the SM value with an uncertainty of 50%. The overall fitted value, $\mu_{VZ} = 0.9 \pm 0.2$, agrees with the SM expectation of $\mu_{VZ} = 1$ and corresponds to an observed significance of 4.8σ, with an expected significance of 5.1σ.

The profile likelihood fit is then performed with the diboson contributions constrained to their SM values within the uncertainties specified ithese proceedings and with the Higgs boson signal strength μ as a free parameter ("Higgs-boson fit"). Figure 1 shows the m_{bb} distributions in some of the signal regions, with background normalisations, signal normalisation, and nuisance parameters adjusted by the Higgs-boson fit. Agreement between data and estimated background is observed within the uncertainties shown by the hashed bands.

The fitted value of the signal strength parameter is $\mu = 0.2 \pm 0.5(\mathrm{stat.}) \pm 0.4(\mathrm{syst.})$ for $m_H = 125$ GeV. Fitted μ values are shown in Fig. 2 for the 7 TeV, 8 TeV and

[1] The NLO corrections to gluon-induced ZH production [32], which increase the total ZH production cross section by about 5%, are not included.

combined datasets, and for the three channels separately and combined. Figure 3 shows the m_{bb} distribution in data after subtraction of all backgrounds except for diboson production. The diboson contribution is clearly seen, located at the expected Z mass. The Higgs boson signal contribution is shown both with its fitted signal strength and as expected for the SM cross section.

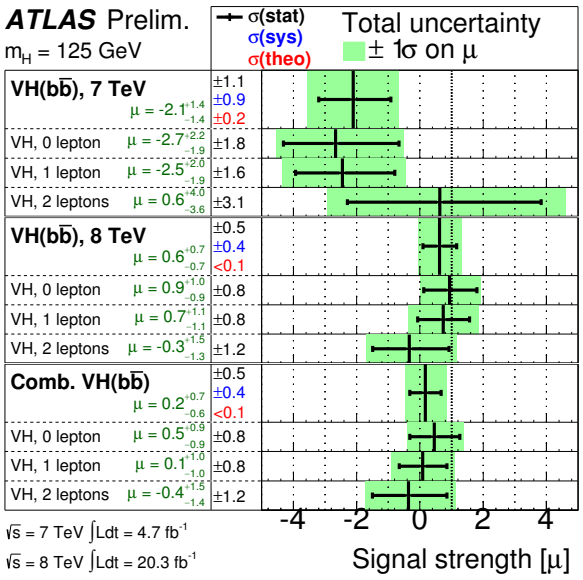

Figure 2: The fitted values of the Higgs-boson signal strength parameter μ for the 7 TeV, 8 TeV, and combined datasets, and for the three channels separately and combined, all for $m_H = 125$ GeV [14]. The individual μ-values for the lepton channels are obtained from a simultaneous fit with the signal strength for each floating independently.

Figure 4 shows the results for the 95% CL upper limits on the Higgs boson production cross section in the mass range 100–150 GeV. No significant excess is observed. The observed limit for $m_H = 125$ GeV is 1.4 times the SM Higgs-boson production cross section, to be compared to an expected limit, in the absence of signal, of 1.3. If the analysis is restricted to the 7 TeV or 8 TeV dataset, the observed (expected) limits are 2.0 (3.3) and 1.9 (1.3), respectively. For the full dataset and all channels combined, the probability p_0 of obtaining a result at least as signal-like as observed if no signal is present is calculated using $q_0 = -2\ln(\mathcal{L}(0, \hat{\hat{\theta}}_\mu)/\mathcal{L}(\hat{\mu}, \hat{\theta}))$ as test statistics. For $m_H = 125$ GeV, the observed p_0 value is 0.36, to be compared to an expectation of 0.05 in the presence of a SM Higgs boson with that mass. The probability for obtaining a result more background-like than observed in the presence of a SM signal ($\mu = 1$) is 0.11.

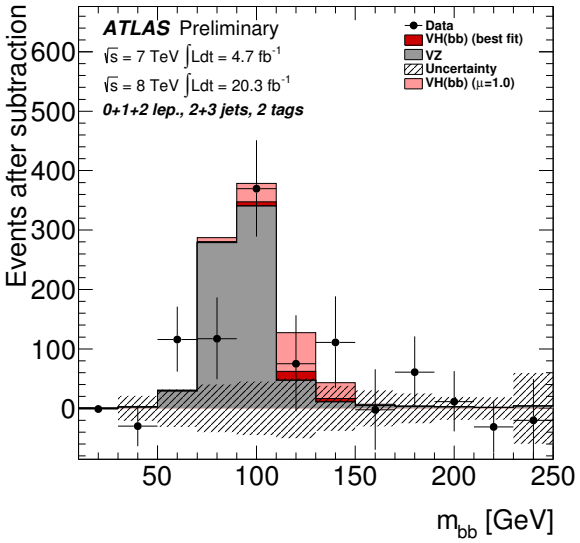

Figure 3: The m_{bb} distribution in data after subtraction of all backgrounds except for the diboson processes and for the associated WH and ZH production of a SM Higgs boson with $m_H = 125$ GeV [14]. The Higgs boson signal contribution is shown both with its fitted signal strength (indicated as "best fit") and as expected for the SM cross section (indicated as $\mu = 1.0$). The size of the combined statistical and systematic uncertainty on the fitted background is indicated by the hashed band.

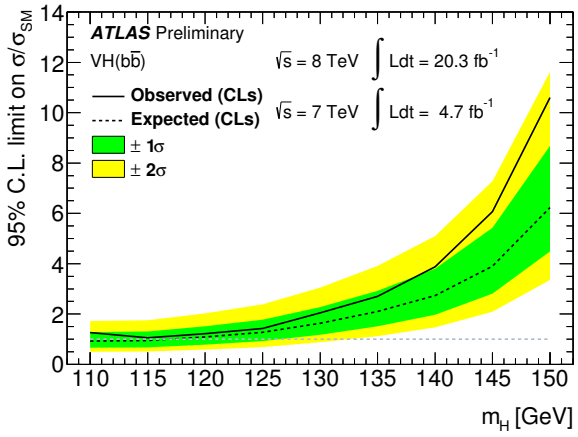

Figure 4: Expected (dashed) and observed (solid) 95% CL cross section upper limits, normalised to the SM Higgs boson production cross section, as a function of m_H for all channels and data taking periods combined [14]. The expected upper limit is given for the background-only hypothesis. The green and yellow bands represent the 1σ and 2σ ranges of the expectation in the absence of a signal.

Aknowledges

Part of this work made in the ILP LABEX (under reference ANR-10-LABX-63) was supported by French state funds managed by the ANR within the Investissements d'Avenir programme under reference ANR-11-IDEX-0004-02.

References

[1] ATLAS Collaboration, *Observation of a new particle in the search for the Standard Model Higgs boson with the ATLAS detector at the LHC*, Phys.Lett. **B716** (2012) 1–29, arXiv:1207.7214.

[2] CMS Collaboration, *Observation of a new boson at a mass of 125 GeV with the CMS experiment at the LHC*, Phys.Lett. **B716** (2012) 30–61, arXiv:1207.7235.

[3] F. Englert and R. Brout, *Broken Symmetry and the Mass of Gauge Vector Mesons*, Phys. Rev. Lett. **13** (1964) 321.

[4] P. W. Higgs, *Broken Symmetries and the Masses of Gauge Bosons*, Phys. Rev. Lett. **13** (1964) 508.

[5] P. W. Higgs, *Broken Symmetries, Massless Particles and Gauge Fields*, Phys. Lett. **12** (1964) 132.

[6] G. Guralnik, C. Hagen, and T. Kibble, *Global Conservation Laws and Massless Particles*, Phys. Rev. Lett. **13** (1964) 585.

[7] S. L. Glashow, *Partial Symmetries of Weak Interactions*, Nucl. Phys. **22** (1961) 579–588.

[8] S. Weinberg, *A Model of Leptons*, Phys. Rev. Lett. **19** (1967) 1264–1266.

[9] A. Salam, *Weak and electromagnetic interactions*, Proc. of the 8th Nobel Symposium (1969) 367.

[10] A. Djouadi, J. Kalinowski, and M. Spira, *HDECAY: A program for Higgs boson decays in the Standard Model and its supersymmetric extension*, Comput. Phys. Commun. **108** (1998) 56–74, arXiv:hep-ph/9704448.

[11] ATLAS Collaboration, *Search for the Standard Model Higgs boson produced in association with a vector boson and decaying to a b-quark pair with the ATLAS detector*, Phys.Lett. **B718** (2012) 369–390, arXiv:1207.0210.

[12] ATLAS Collaboration, *Search for the Standard Model Higgs boson produced in association with a vector boson and decaying to bottom quarks with the ATLAS detector*, ATLAS-CONF-2012-161 (2012), https://cds.cern.ch/record/1493625.

[13] ATLAS Collaboration, *The ATLAS Experiment at the CERN Large Hadron Collider*, JINST **3** (2008) S08003.

[14] ATLAS Collaboration, *Search for the $b\bar{b}$ decay of the Standard Model Higgs boson in associated (W/Z)H production with the ATLAS detector*, ATLAS-CONF-2013-079, http://cds.cern.ch/record/1563235.

[15] ATLAS Collaboration, *Search for the $b\bar{b}$ decay of the Standard Model Higgs boson in associated (W/Z)H production with the ATLAS detector*, arXiv:1409.6212.

[16] ATLAS Collaboration, *Electron performance measurements with the ATLAS detector using the 2010 LHC proton-proton collision data*, Eur. Phys. J **C72** (2012) 1909, arXiv:1110.3174v2.

[17] ATLAS Collaboration, *Measurement of the $W \to \ell\nu$ and $Z/\gamma^* \to \ell\ell$ production cross sections in proton-proton collisions at $\sqrt{s} = 7$ TeV with the ATLAS detector*, JHEP **1012** (2010) 060, arXiv:1010.2130.

[18] M. Cacciari, G. P. Salam, and G. Soyez, *The anti-k_t jet clustering algorithm*, JHEP **04** (2008) 063, arXiv:0802.1189.

[19] ATLAS Collaboration, *Jet energy measurement with the ATLAS detector in proton-proton collisions at $\sqrt{s} = 7$ TeV*, Eur.Phys.J. **C73** (2013) 2304, arXiv:1112.6426.

[20] ATLAS Collaboration, *Measuring the b-tag efficiency in a top-pair sample with 4.7 fb^{-1} of data from the ATLAS detector*, ATLAS-CONF-2012-097 (2012), https://cds.cern.ch/record/1460443.

[21] ATLAS Collaboration, *Performance of Missing Transverse Momentum Reconstruction in Proton-Proton Collisions at 7 TeV with ATLAS*, Eur.Phys.J. **C72** (2012) 1844, arXiv:1108.5602.

[22] ATLAS Collaboration, *The ATLAS Simulation Infrastructure*, Eur. Phys. J **C70** (2010) 823, arXiv:1005.4568.

[23] GEANT4 Collaboration, S. Agostinelli et al., *GEANT4: A Simulation toolkit*, Nucl.Instrum.Meth. **A506** (2003) 250–303.

[24] T. Gleisberg et al., *Event generation with SHERPA 1.1*, JHEP **02** (2009) 007, arXiv:0811.4622.

[25] P. Nason, *A New method for combining NLO QCD with shower Monte Carlo algorithms*, JHEP **0411** (2004) 040, arXiv:hep-ph/0409146.

[26] S. Frixione, P. Nason, and C. Oleari, *Matching NLO QCD computations with Parton Shower simulations: the POWHEG method*, JHEP **0711** (2007) 070, arXiv:0709.2092.

[27] S. Alioli, P. Nason, C. Oleari, and E. Re, *A general framework for implementing NLO calculations in shower Monte Carlo programs: the POWHEG BOX*, JHEP **1006** (2010) 043, arXiv:1002.2581.

[28] T. Sjöstrand, S. Mrenna, and P. Z. Skands, PYTHIA *6.4 Physics and Manual*, JHEP **05** (2006) 026, arXiv:hep-ph/0603175.

[29] B. P. Kersevan and E. Richter-Was, *The Monte Carlo event generator AcerMC version 2.0 with interfaces to PYTHIA 6.2 and HERWIG 6.5*, arXiv:hep-ph/0405247.

[30] G. Corcella et al., *HERWIG 6: an event generator for hadron emission reactions with interfering gluons (including super-symmetric processes)*, JHEP **0101** (2001) 010.

[31] T. Sjöstrand, S. Mrenna, and P. Z. Skands, *A Brief Introduction to PYTHIA 8.1*, Comput.Phys.Commun. **178** (2008) 852–867, arXiv:0710.3820.

[32] L. Altenkamp, S. Dittmaier, R. V. Harlander, H. Rzehak, and T. J. Zirke, *Gluon-induced Higgs-strahlung at next-to-leading order QCD*, JHEP **1302** (2013) 078, arXiv:1211.5015.

[33] J. Ohnemus and W. J. Stirling, *Order α_s corrections to the differential cross-section for the WH intermediate mass Higgs signal*, Phys. Rev. **D47** (1993) 2722–2729.

[34] H. Baer, B. Bailey, and J. F. Owens, *$O(\alpha_s)$ Monte Carlo approach to W+Higgs associated production at hadron supercolliders*, Phys. Rev. **D47** (1993) 2730–2734.

[35] O. Brein, A. Djouadi, and R. Harlander, *NNLO QCD corrections to the Higgs-strahlung processes at hadron colliders*, Phys.Lett. **B579** (2004) 149–156, arXiv:hep-ph/0307206.

[36] M. Ciccolini, S. Dittmaier, and M. Kramer, *Electroweak radiative corrections to associated WH and ZH production at hadron colliders*, Phys.Rev. **D68** (2003) 073003, arXiv:hep-ph/0306234.

[37] A. Denner, S. Dittmaier, S. Kallweit, and A. Mück, *EW corrections to Higgs strahlung at the Tevatron and the LHC with HAWK*, PoS **EPS-HEP2011** (2011) 235, arXiv:1112.5258.

[38] A. L. Read, *Presentation of search results: The CL(s) technique*, J.Phys. **G28** (2002) 2693–2704.

[39] G. Cowan et al., *Asymptotic formulae for likelihood-based tests of new physics*, Eur. Phys. J. **C71** (2011) 1554.